

# **IEICE** **TRANSACTIONS**

## **on Communications**

**VOL. E106-B NO. 1**  
**JANUARY 2023**

**The usage of this PDF file must comply with the IEICE Provisions on Copyright.**

**The author(s) can distribute this PDF file for research and educational (nonprofit) purposes only.**

**Distribution by anyone other than the author(s) is prohibited.**

**A PUBLICATION OF THE COMMUNICATIONS SOCIETY**



The Institute of Electronics, Information and Communication Engineers  
Kikai-Shinko-Kaikan Bldg., 5-8, Shibakoen 3chome, Minato-ku, TOKYO, 105-0011 JAPAN

PAPER

# ECG Signal Reconstruction Using FMCW Radar and a Convolutional Neural Network for Contactless Vital-Sign Sensing\*

Daiki TODA<sup>†</sup>, Ren ANZAI<sup>†</sup>, *Student Members*, Koichi ICHIGE<sup>†a)</sup>, *Member*, Ryo SAITO<sup>††</sup>,  
and Daichi UEKI<sup>††</sup>, *Nonmembers*

**SUMMARY** A method of radar-based contactless vital-sign sensing and electrocardiogram (ECG) signal reconstruction using deep learning is proposed. A radar system is an effective tool for contactless vital-sign sensing because it can measure a small displacement of the body surface without contact. However, most of the conventional methods have limited evaluation indices and measurement conditions. A method of measuring body-surface-displacement signals by using frequency-modulated continuous-wave (FMCW) radar and reconstructing ECG signals using a convolutional neural network (CNN) is proposed. This study conducted two experiments. First, we trained a model using the data obtained from six subjects breathing in a seated condition. Second, we added sine wave noise to the data and trained the model again. The proposed model is evaluated with a correlation coefficient between the reconstructed and actual ECG signal. The results of first experiment show that their ECG signals are successfully reconstructed by using the proposed method. That of second experiment show that the proposed method can reconstruct signal waveforms even in an environment with low signal-to-noise ratio (SNR).

**key words:** *frequency-modulated continuous-wave radar, convolutional neural network, electrocardiogram, heartbeat*

## 1. Introduction

Vital-sign monitoring — which is a key part of managing people’s health — is attracting much attention in the medical and health-care fields. In particular, monitoring heartbeat signals can detect cardiac diseases as well as evaluate levels of fatigue and drowsiness [1], [2]. Electrocardiogram (ECG) signals, which record electrical responses of the heartbeat, and photoplethysmography (PPG) signals, which record changes in the volume of blood vessels, are among the most-common ways to measure heartbeat signals [3]. However, these measurements usually require multiple measurement devices to be in contact with the skin. They are thus unsuitable for (i) monitoring of people with skin problems (such as rashes or burns) or long-term monitoring (such as during sleep or driving) due to the discomfort of contact, and (ii) monitoring of a large number of people due to the risk of infections such as COVID-19 [4], [5].

Vital-sign-sensing methods using radars [6]–[9] and

optical cameras [10]–[12] to achieve contactless heartbeat monitoring have already been investigated. In addition to their ability to acquire the displacement signals from subjects without contact, radar methods can protect privacy and measure signals regardless of ambient brightness [13], [14]. Heartbeat signals have a very small amplitude compared to noise such as respiration and body motion, so it is not easy to extract their component from the displacement signals acquired by radar. Most radar-based methods therefore aim to estimate heart rate (HR) and R-R interval (RRI), which represents the interval between heartbeats. However, in addition to the most-remarkable R-peak, features such as the P-wave and T-wave may make it possible to detect cardiac diseases, and more detailed features of heartbeats can be obtained if waveforms of ECG signals could be reconstructed. Doppler radar and deep-learning models have been used to reconstruct ECG signals [9], and other approaches have reconstructed ECG signals by using contact devices such as PPG sensors [3], [15], [16]. The motivation of using deep-learning technique is, as discussed in [6], the learning-based methods are good at extracting features of heartbeat signals while the linear approaches often fail to distinguish heartbeat from breathing signals.

In consideration of actual environments of heartbeat monitoring by a radar device, it is not desirable to impose a stationary state on subjects. In situations in which the subject’s body is moving [17], for example, the device is used as a driver-monitoring system (DMS) [2], or the device is fixed to a moving object such as a drone [18], low signal-to-noise ratio (SNR) often becomes a problem due to vibration and other noise factors. A method to classify signals with high SNR [19] and improve heartbeat-estimation accuracy when using radar in a low-SNR situation has been proposed, but it has not yet been applied to the problem of reconstructing ECG signals.

In response to the above-described circumstances, we propose a method for (i) acquiring a signal representing displacement of the body surface by using frequency-modulated continuous-wave (FMCW) radar and (ii) reconstructing reference ECG signals (acquired by a contact sensor) by using a convolutional neural network (CNN). The body-surface-displacement signal is modified into two dimensions and differentiated in a preprocessing step. It is then used as an input to the CNN to estimate the normalized ECG signals. We then trained the CNN on the radar signals with various strengths and frequencies of noises added, and we confirmed

Manuscript received January 17, 2022.

Manuscript revised April 25, 2022.

Manuscript publicized June 29, 2022.

<sup>†</sup>The authors are with Department of Electrical and Computer Engineering, Yokohama National University, Yokohama-shi, 240-8501 Japan.

<sup>††</sup>The authors are with Murata Manufacturing Co., Ltd., Nagaokakyo-shi, 617-8555 Japan.

\*Preliminary version of this paper is presented in [23], [24].

a) E-mail: koichi@ynu.ac.jp

DOI: 10.1587/transcom.2022EBP3005

that the CNN could accurately reconstruct the ECG signals. We adopted a correlation coefficient with actual ECG signals as an evaluation metric, and we calculated the value of RRI by using an existing RRI estimation algorithm [20] and evaluated its mean absolute error (MAE). The main contribution of this paper is as follows.

- We dealt with the problem of ECG signal reconstruction, and developed a novel model which can reconstruct the signal as accurate as the conventional methods under a stationary state.
- As an initial study, we investigated an environment with low SNR; case of signals with additive sine wave noise.

## 2. Conventional Methods

Conventional methods related to this study are briefly introduced hereafter. Many methods for reconstructing waveforms of ECG signals are based on contact sensors such as those using PPG. For example, methods for reconstructing ECG signals from PPG signals by using a discrete cosine transform (DCT) [3], dictionary learning [15], and a transformed attentional neural network (which is one representative deep-learning model [16]) have been proposed. However, all of those methods require contact devices to measure ECG signals.

In contrast to waveform-reconstruction methods for ECG signals, most methods for detecting heartbeats by using radar focus on R-peaks. One such method [7] uses convolutional long short-term memory (LSTM) to construct a model that takes a time-frequency representation of radar signal as input, gives a band-pass filtered ECG signal as an output, and calculates RRI by peak detection. Another method [6] creates two triangular waves whose maxima match R and S-peaks, and triangular waves are estimated from the radar signals by using a CNN and a recurrent neural network (RNN) combined model. Another approaches estimates RRI by inputting certain parts of filtered radar signals, classifying whether a region contains a heartbeat, and then detecting a peak in the region with a heartbeat component [21]. Another method uses differential arithmetic, a band-pass filter, and a Kalman filter [13]. Although these methods can detect heartbeat intervals, they reduce detailed features of ECG signals, so they are not preferable for advanced feature extraction with detailed information of heartbeats.

A few methods for reconstructing an ECG signal use radar signals. One method using Doppler radar and deep-learning models has been proposed [9]. As for that method, filtered in-phase and quadrature-phase (IQ) signals are both used as input, and the ECG waveform is reconstructed by using a CNN and LSTM model. RRI is then calculated from the reconstructed ECG signal by using an existing method of detecting the R-peak.

Although most radar methods are based on Doppler radar [1], [4], [6]–[9], some of them are based on FMCW radar [13], [17]. A method considering external environmental noises from cars, trains, airplanes, and also from

men’s body movement, other than breathing has not been investigated. So it is important to consider the extent to which the reconstruction result can be guaranteed in a low-SNR environment.

## 3. Proposed Method

The proposed method of measuring body-surface-displacement signals by using FMCW radar and reconstructing ECG signals by using a CNN model is described hereafter. The proposed method can be divided into two schemes: in the first, body-surface displacement is measured; and in the second, the signal is reconstructed. The overall configuration of a system based on the proposed is shown in Fig. 1. Note that the difference between the proposed method and the method [9] are as follows.

- We developed the method of reconstructing ECG signals only by CNN, while the method [9] did not. We did not use recursive construction and therefore could reduce the computational cost.
- The estimation accuracy of the proposed method is comparable with that in [9] even with lower computational cost.
- We added not only breathing signals but also noises.

### 3.1 Displacement Measurement Using FMCW Radar

The method for measuring a body-surface-displacement signal by FMCW radar is described first. A FMCW radar transmits a signal whose frequency varies linearly with time (a so-called “chirp” signal) at transmission point Tx, and receives the signal reflected from the subject’s body surface at reception point Rx, as shown in the upper part of Fig. 1. Phase information is then extracted by a mixer and range fast Fourier transform (FFT), and the displacement is calculated from the amount of phase change in each chirp. The frequency of the  $k$ -th chirp signal can be expressed as

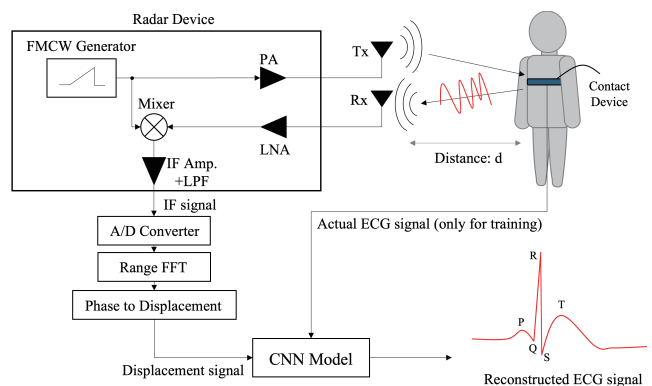


Fig. 1 Overview of system.

$$f_k(t) = \begin{cases} f_{\min} + \frac{B}{T_c}(t - kT_c), & kT_c < t < (k+1)T_c, \\ 0, & \text{otherwise,} \end{cases} \quad (1)$$

where  $f_{\min}$  is the lowest frequency,  $T_c$  is chirp interval, and  $B$  is frequency bandwidth.

The radio wave transmitted from Tx is received at Rx after round trip time  $\tau = 2d/c$  with distance  $d$  and the speed of light  $c$ . An intermediate-frequency (IF) signal is then generated by a mixer and is expressed as

$$s_{\text{IF},k}(t) = \frac{A_t A_r}{2} \exp\left(j2\pi\left\{\frac{B}{T_c}\tau(t - kT_c) - \frac{B}{T_c}\tau^2 + \tau f_{\min}\right\}\right), \quad (2)$$

where  $A_t$  and  $A_r$  are the amplitudes of the transmitted and received signals, respectively. After A/D conversion, the body-surface displacement can be obtained as

$$s_d(k) = \mathcal{L}\mathcal{F}\left[s_{\text{IF},k}(t)\right](f_d) \cdot \frac{c}{4\pi f_{\min}}, \quad (3)$$

where  $\mathcal{F}[\cdot]$  denotes the range FFT, and the desired frequency is set to  $f_d$ .

As for the proposed method, a 79-GHz FMCW radar with one Tx element and one Rx element is used. Frequency bandwidth is 3.2 GHz, and sampling frequency of body-surface displacement is 66.7 Hz.

### 3.2 ECG Signal Reconstruction by CNN

Reference [6] proposed an deep-learning model using CNN/RNN and triangular waves, and could extract the characteristics of signals in a long-time span. However, their approach seems to lose minute characteristics and requires large computational cost due to RNN [22]. Hence we develop a deep-learning method using the CNN with convolution and fully connected layers.

The proposed CNN model is described as follows. In the case of time-series signals, features including relationships with neighboring points are usually obtained by one-dimensional convolution. The  $i$ -th signal sample in the  $(\ell + 1)$ -th layer input  $x_i^{\ell+1}$  is computed by using a kernel of size  $P$  as follows:

$$x_i^{\ell+1} = h\left(\sum_{p=0}^{P-1} w_p x_{i+p}^{\ell}\right), \quad (4)$$

where  $h(\cdot)$  is an activation function and  $w$  is a weight. According to (4), the convolution operation only uses the data of  $P$  points per layer. It is thus difficult to extract features that relate the information of neighboring heartbeats, if the frequency of the heartbeat signals is sufficiently smaller than the sampling frequency of the body-surface displacement. Therefore, as for the proposed model, a one-dimensional signal  $x_i$  are rearranged into a two-dimensional signal, with

height  $H$  and width  $W$ , denoted by  $\tilde{x}_{i,j}$ . A two-dimensional convolution operation is then applied to  $\tilde{x}_{i,j}$  by using a kernel with size of  $P \times Q$  as follows:

$$\tilde{x}_{i,j}^{\ell+1} = h\left(\sum_{p=0}^{P-1} \sum_{q=0}^{Q-1} w_{p,q} \tilde{x}_{i+p,j+q}^{\ell}\right), \quad (5)$$

where  $\tilde{x}_{i,j} = x_{i+Hj}$ . According to (5), it is possible to learn relationships not only between neighboring points but also between points that are a little far apart.

The constructed two-dimensional CNN model with three convolutional layers and three fully connected layers is shown in Fig. 2. The input signal is preprocessed by

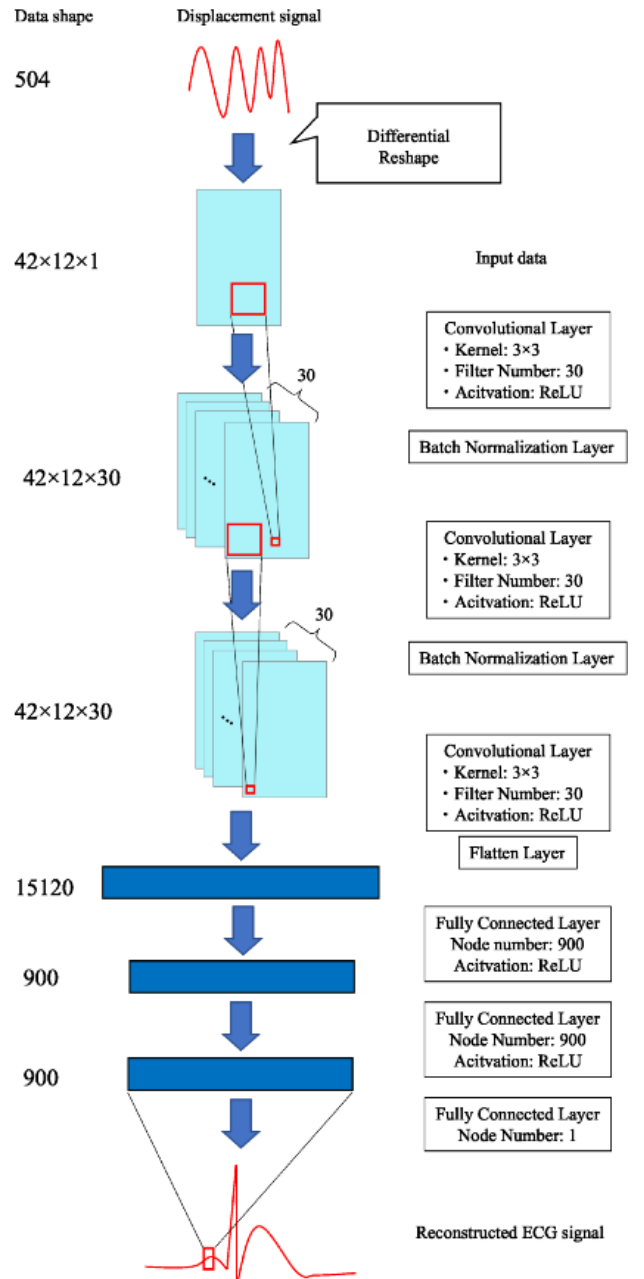


Fig. 2 Overview of CNN architecture.

first-order differentiation. The preprocessed signal is then extracted at a fixed time according to input size  $H \times W$  and rearranged into two dimensions so that we can learn from the input data in a wide range at a same time. The size of the input signal is  $12 \times 42$ . The number of filters in the convolutional layer is 30, and the kernel size is  $3 \times 3$ . Each convolutional layer and fully connected layer (except the output layer) uses a rectified linear unit (ReLU) function as the activation function. The convolutional layers are interspersed with batch-normalization layers to normalize the data in each batch. The number of nodes in all the fully connected layers is set to 900, and the output signal is the normalized ECG signal. Note that the output becomes just one sample of ECG signal, because the output node number of the final output layer is one. Mean square error (MSE) is used for the loss function, and the algorithm Adam is used for the optimization function.

The model structure has been empirically determined, while adjusting the number of convolution and fully connected layers, and inserting pooling and Batch Normalization layers. We found that the pooling layer often eliminated the features and therefore we did not insert the pooling later in the proposed model structure. The model parameters have been optimized by using the library “optuna”, an automatic hyperparameter optimization software framework.

Note that we use the data from one subject in both training and testing, as the conventional work [6] was using the data in a similar manner. Indeed we assume a situation to monitor one subject for a long time, for example, during sleeping or driving and try to detect abnormalities. It would also be valuable to learn data of multiple subjects at a same time, and separate the subjects to be used as training and testing data. That could be applicable to personal identification applications, which is left as one of future subjects.

## 4. Experiments

The ECG signal was experimentally reconstructed in two experiments. In the first experiment, “experiment I”, we investigated whether it is possible to reconstruct the waveform of an ECG signal by using signals acquired by an FMCW radar with the subject in stationary state. In the second experiment, “experiment II”, experiment I was repeated with artificial noise added to the radar signal.

Hereafter, the detailed specifications of the experiments are described first, and the results of experiment I are then presented. After that, the results of investigating noisy cases in experiment II are presented.

### 4.1 Specifications of Experiments

The subjects of the experiments were six adult-male subjects (A to F) without heart disease, and their heartbeats when breathing in a relaxed state were measured (for 5 min) by a contact ECG sensor attached to the chest. Each subject’s heartbeat was also measured by radar. The sampling frequency of the contact sensor was 250 Hz, and the signal

**Table 1** Radar specifications.

| modulation method  | FMCW          |
|--------------------|---------------|
| detection range    | 5 to 10 cm    |
| subjects           | 6 adult males |
| sampling frequency | 66.7 Hz       |

was resampled to 66.7 Hz as the ground truth for the CNN. The radar apparatus was placed behind the back of the chair in which the subject were sitting and aimed at their back, where the distance  $d$  from the apparatus to the chair in Fig. 1 was roughly about ten centimeters. Radar specifications are summarized in Table 1.

The measured data for each subject were divided into three-subsets. 70% (210 s) of each subject’s data was used as training dataset, 10% (30 s) as validation dataset, and 20% (60 s) as test dataset. The differential signal based on the displacement data was then used as the input to the CNN. Furthermore, a reported method for detecting RRI [20] was applied to the reconstructed ECG signal after estimation of CNN.

Correlation coefficient  $\rho$  between the reconstructed and actual ECG signals is defined as

$$\rho = \frac{\sum_{m=1}^M (y_m - \bar{y})(\hat{y}_m - \bar{\hat{y}})}{\sqrt{\sum_{m=1}^M (y_m - \bar{y})^2} \sqrt{\sum_{m=1}^M (\hat{y}_m - \bar{\hat{y}})^2}}, \quad (6)$$

and calculated as an evaluation metric, where  $M$  is the number of all sample points, and  $y_m$  and  $\hat{y}_m$  are the estimated and measured values of the  $m$ -th point of the ECG signal, respectively. Moreover,  $\bar{y}$  and  $\bar{\hat{y}}$  are their mean values.

Estimated RRI is evaluated by using mean  $\mu$ , and standard deviation  $\sigma$  and the MAE are respectively defined as

$$\mu = \frac{1}{N} \sum_{n=1}^N \text{RRI}_{\text{pred}}(n), \quad (7)$$

$$\sigma = \sqrt{\frac{1}{N} \sum_{n=1}^N (\text{RRI}_{\text{pred}}(n) - \mu)^2}, \quad (8)$$

$$\text{MAE} = \frac{1}{N} \sum_{n=1}^N |\text{RRI}_{\text{pred}}(n) - \text{RRI}_{\text{ref}}(n)|, \quad (9)$$

where  $N$  represents the number of all R-peaks in the each subject’s subset, and  $\text{RRI}_{\text{pred}}$  and  $\text{RRI}_{\text{ref}}$  are the predicted (reconstructed) and the reference (actual) RRIs, respectively.

### 4.2 Experiment I

First, in experiment I, an ECG signal was experimentally reconstructed in stationary state. Correlation coefficient and RRI for each subject are summarized in Table 2, and the waveforms for subjects A, C, and E are shown in Fig. 3 as examples of the reconstructed ECG signals. According to

**Table 2** Behavior of correlation coefficient  $\rho$  and RRI in experiment I.

| Subject | $\rho$ | MAE   | RRI [ms]     |          |            |          |
|---------|--------|-------|--------------|----------|------------|----------|
|         |        |       | Reconst. ECG |          | Actual ECG |          |
|         |        |       | $\mu$        | $\sigma$ | $\mu$      | $\sigma$ |
| A       | 0.806  | 58.2  | 772.8        | 30.4     | 797.3      | 32.6     |
| B       | 0.825  | 134.8 | 643.1        | 43.2     | 658.3      | 28.8     |
| C       | 0.957  | 118.1 | 829.1        | 52.2     | 830.8      | 24.3     |
| D       | 0.831  | 50.9  | 738.9        | 27.6     | 736.0      | 30.5     |
| E       | 0.894  | 133.4 | 911.8        | 115.1    | 909.4      | 72.1     |
| F       | 0.852  | 117.6 | 598.6        | 26.5     | 593.5      | 27.0     |
| Average | 0.861  | 102.2 | —            | —        | —          | —        |

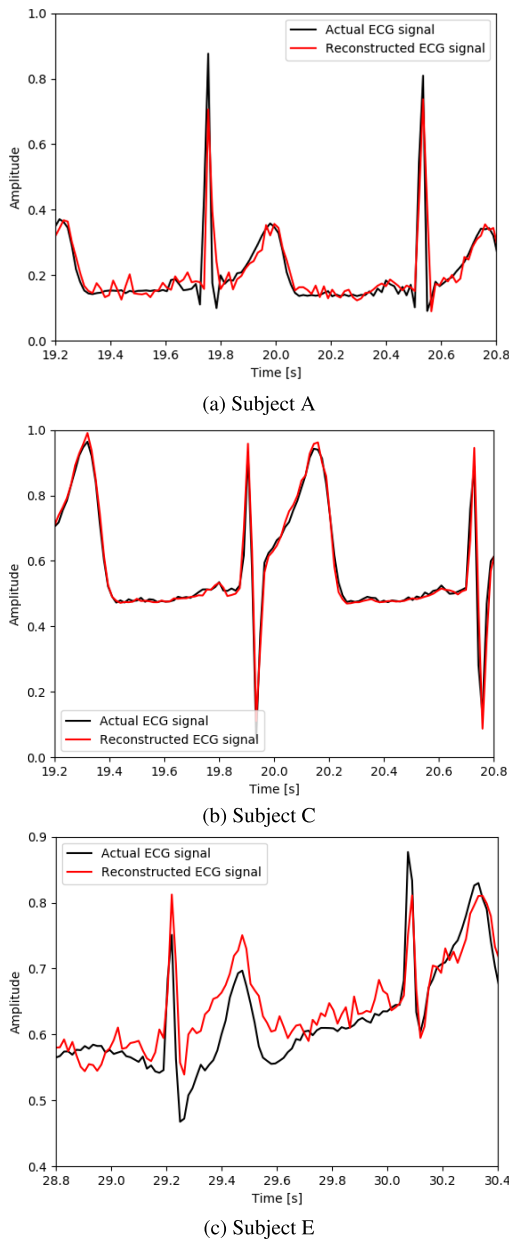


**Fig. 3** Behavior of actual and reconstructed signals in experiment I.

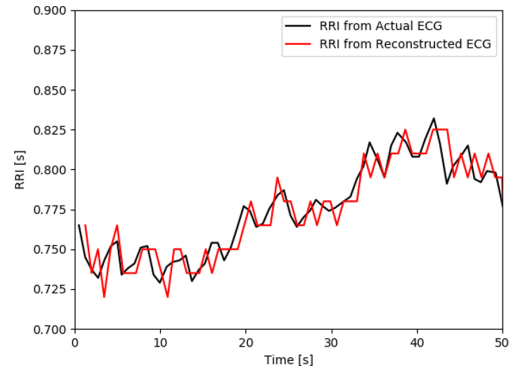


**Fig. 4** Behavior of actual and estimated RRIs in experiment I (subject A).

the table and figure, that the correlation coefficient exceeds 0.80 for all the subjects, and that result confirms that the ECG signal could be accurately reconstructed. Also, Fig. 4 shows that the mean and standard deviation of RRI were estimated accurately. Table 2 and Fig. 3 confirm that correlation coefficient  $\rho$  is large for subject C, because the R-peak is lower and the T-peak is higher than those of the other subjects. It is also clear that standard deviation  $\sigma$  is large for subject E, whose baseline potential fluctuates as shown in Fig. 3(c). One of the reasons for the variation in estimation accuracy among the subjects is that the ECG waveform differs greatly from subject to subject. In addition, the ECG waveform shows different characteristics depending on sweating, breathing depth, blood pressure, and many other conditions. The reference ECG waveforms may have been affected by the fixed position of the contact device, which is normally attached to a specific position on the body of each subject when acquiring ECG waveforms.

Averaged correlation coefficient  $\rho$  and averaged MAE of the conventional [9] and proposed methods are compared in Table 3. It is clear from the table that the correlation coefficients are the same, indicating that the proposed method is as accurate as the conventional method [9]. However, MAE of RRI estimated by the proposed method is much higher than that estimated by the conventional method [9]. This is because the sampling frequency of the conventional method is 1,000 Hz, while that of the proposed method is 66.7 Hz; that is, the difference in sampling frequency was around 15 times. As a result, the conventional method gives an error of 1 ms when the estimated R-peak has an error of just one sample, but the proposed method gives an error of 15 ms. This large error can be reduced by introducing a system for acquiring body-surface displacement with a higher sampling rate.

### 4.3 Experiment II

#### 4.3.1 Adding Artificial Vibration Noise

In case that the proposed measurement system (a subject and the radar device) vibrates, the measurement of the displacement waveform by radar may be less accurate due to the

**Table 3** Comparison of averaged correlation coefficient  $\rho$  and averaged MAE.

| Methods         | $\rho$ | MAE [ms] |
|-----------------|--------|----------|
| Ref. [9]        | 0.86   | 17.8     |
| Proposed method | 0.86   | 102.2    |

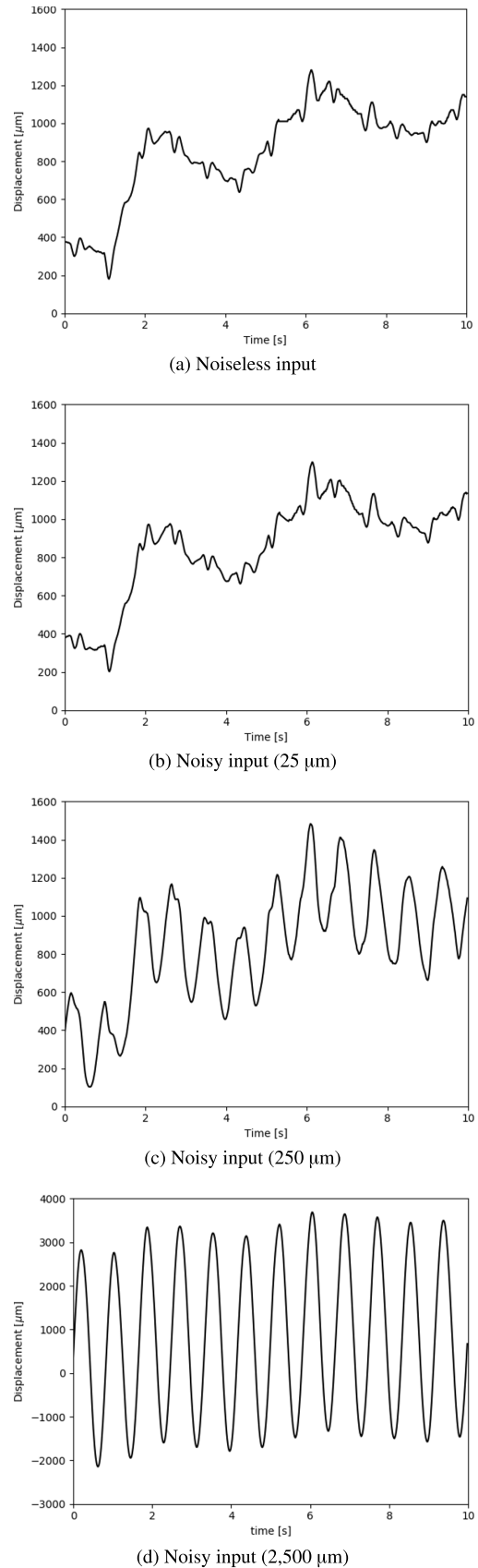
inclusion of undesired noisy components such as reflected waves from the subject's skin at non-target points. Accordingly, instead of re-measuring the displacement waveform when the system was under vibration, we added artificial sine wave noise to the measured data when the system was in stationary state, in which the frequency overlaps the overtone component of the heartbeat and the amplitude is larger than that of the heartbeat. This is because we want to investigate how much they affect the accuracy of the proposed deep-learning model in an environment in which only SNR is degraded.

In an actual environment, various kinds of noises will be added to observed signals. However, there have not been any conventional work how much noises affect to the accuracy of vital-sign sensing using machine learning. Therefore, as an initial study, we added a sine wave noise whose frequency and amplitude are known in advance, and investigated which frequency and/or amplitude affects to the accuracy of signal reconstruction.

Frequency range of a normal heartbeat is generally from 0.5 to 2 Hz at rest [1], and displacement of the body surface caused by the heartbeat is empirically known to be about 10 to 100  $\mu\text{m}$ . In experiment II, sine waves with amplitudes of 25  $\mu\text{m}$ , 250  $\mu\text{m}$ , and 2,500  $\mu\text{m}$  and frequencies of 0.48 Hz, 1.2 Hz, 2.4 Hz, 4.8 Hz, and 12 Hz were added to the displacement signal acquired in experiment I. Examples of Subject A's input signals before and after adding noise signals with different amplitudes but fixed frequency of 1.2 Hz are shown in Fig. 5. It is clear from the figure that displacement due to respiration is large in the case of 25- $\mu\text{m}$  noise; therefore, the displacement signal with 25- $\mu\text{m}$  noise would be similar to the noiseless signal. However, there are fluctuations due to noise in the signal with 250- $\mu\text{m}$  noise as large as respiration, and the noise component is much larger than the noiseless signal in the signal with 2,500- $\mu\text{m}$  noise. How much such noise signals affect estimation accuracy is discussed in the next subsection.

#### 4.3.2 Results of Experiment II

In experiment II, experiment I was repeated with artificial noise added to the radar signal. Values of correlation coefficient  $\rho$  in relation to frequency and amplitude of added noise in experiment II (for subject A and the average for all the subjects) are listed in Tables 4(a) and 4(b). To evaluate the results strictly, the results for subject A are independently shown in Table 4(a) because that subject had the lowest correlation coefficient  $\rho$  of the subjects in experiment I. It is clear from the table that  $\rho$  is large enough in most cases, except the case of large noise amplitude, 2,500  $\mu\text{m}$ , and high noise frequency, 12 Hz. This finding confirms that the ECG

**Fig. 5** Example of noiseless and noisy inputs (1.2 Hz).

**Table 4** Behavior of correlation coefficient  $\rho$  in experiment II.

| (a) subject A        |                                   |       |       |
|----------------------|-----------------------------------|-------|-------|
| Noise Frequency [Hz] | Noise amplitude [ $\mu\text{m}$ ] |       |       |
|                      | 25                                | 250   | 2,500 |
| 0.48                 | 0.800                             | 0.725 | 0.715 |
| 1.2                  | 0.793                             | 0.682 | 0.677 |
| 2.4                  | 0.769                             | 0.677 | 0.779 |
| 4.8                  | 0.737                             | 0.690 | 0.702 |
| 12                   | 0.743                             | 0.761 | 0.028 |

| (b) average for all the subjects |                                   |       |       |
|----------------------------------|-----------------------------------|-------|-------|
| Noise Frequency [Hz]             | Noise amplitude [ $\mu\text{m}$ ] |       |       |
|                                  | 25                                | 250   | 2,500 |
| 0.48                             | 0.849                             | 0.826 | 0.827 |
| 1.2                              | 0.845                             | 0.820 | 0.799 |
| 2.4                              | 0.836                             | 0.822 | 0.569 |
| 4.8                              | 0.826                             | 0.813 | 0.563 |
| 12                               | 0.827                             | 0.837 | 0.302 |

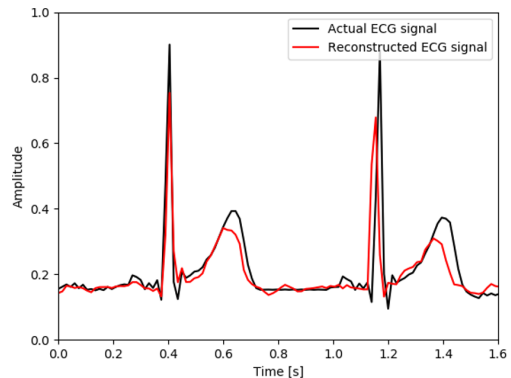
signal could be accurately reconstructed even in the case of noise amplitude of 2,500 $\mu\text{m}$ , which was very large for a heartbeat amplitude and has frequency overlap. We also see that the behavior of the correlation coefficient  $\rho$  for all the subjects in Table 3(b) looks similar to the behavior of that for the subject A in Table 3(a). However, the correlation coefficient  $\rho$  becomes very small for some subjects in case of 2500 $\mu\text{m}$  noise. We confirmed that the very large noise of 2500 $\mu\text{m}$  had affected to the average performance as well.

Behaviors of the actual and reconstructed signals and RRIs in the case of Subject A, 1.2 Hz and 2,500- $\mu\text{m}$  noise are shown in Fig. 6. It is clear from Fig. 6(a) that the reconstructed R-peak and T-wave peaks are slightly lower than the actual ones, indicating that the accuracy of the reconstruction based on the correlation coefficient is lower, but the characteristics of the ECG signal are maintained. Fig. 6(b) shows actual and estimated RRIs. It is clear from the figure that some R-peaks were not detected in the first 15 s because of large noise signals, but RRI in the following period is estimated accurately. So far, we have not determined the reason for the inaccurate estimation result shown in Fig. 6(b) in the first 15 s, so that task remains as part of future studies.

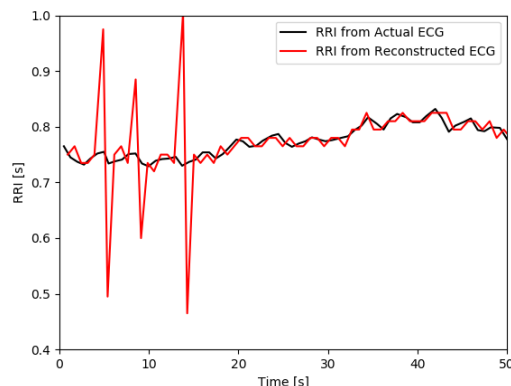
It was also observed that the waveform could not be reconstructed under the condition of large noise frequencies and large noise amplitudes. This result clearly shows that higher frequency and larger displacement will have a greater effect on waveform-reconstruction accuracy than the case that the heartbeat frequency overlaps the noise frequency. Improving reconstruction accuracy under such high-frequency noise also remains as one of our future studies.

## 5. Conclusion

A method of measuring body-surface-displacement signals by using FMCW radar and reconstructing ECG signals by using a CNN was proposed. It was confirmed that the proposed method can reconstruct ECG signals as accurately as the conventional method when the subject is in a stationary condition. Furthermore, the proposed method can recon-



(a) Behavior of actual and reconstructed signals



(b) Behavior of actual and estimated RRIs

**Fig. 6** Behaviors of signals and RRIs in experiment II (in case of 1.2 Hz and 2,500- $\mu\text{m}$  noise).

struct ECG waveforms — even under severe conditions of low SNR — by adding artificial noise signals.

As discussed in Sect. 4, sampling frequency of body-surface displacement should be increased to improve accuracy of the deep-learning model.

The following issues (a)–(d) remain as future studies: (a) develop an improved measurement system with a higher sampling rate, (b) improve the system which can correspond to the ground truth of P and T peaks, (c) learn the data of multiple subject at the same time, and (d) experiments under various kinds of noises.

## Acknowledgments

This work was supported in part by Japan Society for the Promotion of Science (JSPS) Grant-in-Aid for Scientific Research no. 20K04500. The authors are sincerely grateful for their support.

## References

- [1] K. Yamamoto, K. Toyoda, and T. Ohtsuki, “Spectrogram-based Non-contact RRI estimation by accurate peak detection algorithm,” *IEEE Access*, vol.6, pp.60369–60379, Oct. 2018. DOI: 10.1109/ACCESS.2018.2875737
- [2] K. Fujiwara, E. Abe, K. Kamata, C. Nakayama, Y. Suzuki, T. Yamakawa, T. Hiraoka, M. Kano, Y. Sumi, F. Masuda, M. Mat-

- suo, and H. Kadotani, “Heart rate variability-based driver drowsiness detection and its validation with EEG,” *IEEE Trans. Biomed. Eng.*, vol.66, no.6, pp.1769–1778, Nov. 2018. DOI: 10.1109/TBME.2018.2879346
- [3] X. Tian, Q. Zhu, Y. Li, and M. Wu, “Cross-domain joint dictionary learning for ECG reconstruction from PPG,” *Proc. IEEE International Conf. Acoustics, Speech and Signal Processing*, pp.936–940, May 2020. DOI: 10.1109/ICASSP40776.2020.9054242
- [4] V.L. Petrović, M.M. Janković, A.V. Lupšić, V.R. Mihajlović and J.S. Popović-Božović, “High-accuracy real-time monitoring of heart rate variability using 24 GHz continuous-wave Doppler radar,” *IEEE Access*, vol.7, pp.74721–74733, June 2019. DOI: 10.1109/ACCESS.2019.2921240
- [5] T. Sakamoto, S. Mitani, and T. Sato, “Noncontact monitoring of heartbeat and movements during sleep using a pair of millimeter-wave ultra-wideband radar systems,” *IEICE Trans. Commun.*, vol.E104-B, no.4, pp.463–471, April 2021. DOI: 10.1587/transcom.2020EBP3078
- [6] S. Wu, T. Sakamoto, K. Oishi, T. Sato, K. Inoue, T. Fukuda, K. Mizutani, and H. Sakai, “Person-specific heart rate estimation with ultra-wideband radar using convolutional neural networks,” *IEEE Access*, vol.7, pp.168484–168494, Nov. 2019. DOI: 10.1109/ACCESS.2019.2954294
- [7] K. Yamamoto and T. Ohtsuki, “Non-contact heartbeat detection by heartbeat signal reconstruction based on spectrogram analysis with convolutional LSTM,” *IEEE Access*, vol.8, pp.123603–123613, June 2020. DOI: 10.1109/ACCESS.2020.3006107
- [8] W. Xia, Y. Li, and S. Dong, “Radar-based high-accuracy cardiac activity sensing,” *IEEE Trans. Instrum. Meas.*, vol.70, pp.1–13, Jan. 2021. DOI: 10.1109/TIM.2021.3050827
- [9] K. Yamamoto, R. Hiromatsu, and T. Ohtsuki, “ECG signal reconstruction via Doppler sensor by hybrid deep learning model with CNN and LSTM,” *IEEE Access*, vol.8, pp.130551–130560, July 2020. DOI: 10.1109/ACCESS.2020.3009266
- [10] M. van Gastel, S. Stuijk, S. Overeem, J.P. van Dijk, M.M. van Gilst, and G. de Haan, “Camera-based vital signs monitoring during sleep—A proof of concept study,” *IEEE J. Biomed. Health Inform.*, vol.25, pp.1409–1418, Dec. 2020. DOI: 10.1109/JBHI.2020.3045859
- [11] M.F. Ahmed, M.O. Ali, M.H. Rahman, and Y.M. Jang, “Real-time health monitoring system design based on optical camera communication,” *Proc. International Conf. on Information Networking*, pp.870–873, Jan. 2021. DOI: 10.1109/ICOIN50884.2021.9334018
- [12] G. Zhang, S. Zhang, Y. Dai, and B. Shi, “Using rear smartphone cameras as sensors for measuring heart rate variability,” *IEEE Access*, vol.9, pp.20460–20468, Jan. 2021. DOI: 10.1109/ACCESS.2021.3054065
- [13] S. Ji, H. Wen, J. Wu, Z. Zhang, and K. Zhao, “Systematic heartbeat monitoring using a FMCW mm-Wave radar,” *Proc. IEEE International Conf. Consumer Electronics and Computer Engineering*, pp.714–718, Jan. 2021. DOI: 10.1109/ICCECE51280.2021.9342280
- [14] I. Nejadgholi, S. Rajan, and M. Bolic, “Time-frequency based contactless estimation of vital signs of human while walking using PMCW radar,” *Proc. IEEE International Conf. e-Health Networking, Applications and Services*, pp.1–6, Sept. 2016. DOI: 10.1109/HEALTHCOM.2016.7749445
- [15] X. Tian, Q. Zhu, Y. Li, and M. Wu, “ECG reconstruction via PPG: A pilot study,” *Proc. IEEE EMBS International Conf. Biomedical Health Informatics*, pp.1–4, Sept. 2019. DOI: 10.1109/BHI.2019.8834612
- [16] H.Y. Chiu, H.H. Shuai, and P.C.P. Chao, “Reconstructing QRS complex from PPG by transformed attentional neural networks,” *IEEE Sensors J.*, vol.20, no.20, pp.12374–12383, June 2020. DOI: 10.1109/JSEN.2020.3000344
- [17] M. Shibao and A. Kajiwara, “Heart-rate monitoring of moving persons using 79 GHz ultra-wideband radar sensor,” *IEICE Commun. Express*, vol.9, no.5, pp.125–130, Feb. 2020. DOI: 10.1587/comex.2020XBL0005
- [18] S.M.M. Islam, L.C. Lubecke, C. Grado, and V.M. Lubecke, “An adaptive filter technique for platform motion compensation in unmanned aerial vehicle based remote life sensing radar,” *Proc. European Microwave Conf.*, pp.937–940, Jan. 2021. DOI: 10.23919/EuMC48046.2021.9338011
- [19] K. Shi, S. Schellenberger, F. Michler, T. Steigleder, A. Malessa, F. Lurz, C. Ostgathe, R. Weigel, and A. Koelplin, “Automatic signal quality index determination of radar-recorded heart sound signals using ensemble classification,” *IEEE Trans. Biomed. Eng.*, vol.67, no.3, pp.773–785, June 2019. DOI: 10.1109/TBME.2019.2921071
- [20] M. Elgendi, M. Jonkman, and F. DeBoer, “Frequency bands effects on QRS detection,” *Proc. 3rd International Conf. Bio-inspired Systems and Signal Processing*, pp.428–431, Jan. 2010. ISBN: 978-989674018-4
- [21] Y. Li, Z. Xia, and Y. Zhang, “Standalone systolic profile detection of non-contact SCG signal with LSTM network,” *IEEE Sensors J.*, vol.20, pp.3123–3131, Dec. 2019. DOI: 10.1109/JSEN.2019.2957382
- [22] O.I. Abiodun, A. Jantan, A.E. Omolara, K.V. Dada, N.A. Mohamed, and H. Arshad, “State-of-the-art in artificial neural network applications: A survey,” *Heliyon*, vol.4, no.11, e00938, Nov. 2018. DOI: 10.1016/j.heliyon.2018.e00938
- [23] D. Toda, R. Anzai, K. Ichige, R. Saito, and D. Ueki, “ECG signal reconstruction using FMCW radar and convolutional neural network,” *IEICE Society Conference*, no.B-1-84, Sept. 2021 (in Japanese).
- [24] D. Toda, R. Anzai, K. Ichige, R. Saito, and D. Ueki, “ECG signal reconstruction using FMCW radar and convolutional neural network,” *Proc. International Symposium on Communications and Information Technologies*, pp.176–181, Oct. 2021. DOI:10.1109/ISCI52804.2021.9590627



**Daiki Toda** received B.E. and M.E. degrees in Electrical and Computer Engineering from Yokohama National University in 2020 and 2022, respectively. His research interests include deep learning and vital sensing.



**Ren Anzai** received B.E. and M.E. degrees in Electrical and Computer Engineering from Yokohama National University in 2021 and 2023, respectively. His research interests include deep learning and vital sensing.



**Koichi Ichige** received B.E., M.E., and Dr. Eng. degrees in Electronics and Computer Engineering from the University of Tsukuba in 1994, 1996, and 1999. He became a research associate at the Department of Electrical and Computer Engineering, Yokohama National University in 1999, where he is currently a professor. He was a visiting researcher at the Swiss Federal Institute of Technology Lausanne (EPFL), Switzerland, in 2001–2002. His research interests include digital signal processing, approximation theory, and their applications to image processing and mobile communication.

He served as an associate editor of *IEEE Transactions on Industrial Electronics* in 2004–2008, an associate editor of *Journal of Circuits, Systems and Computers (JCSC)* in 2012–2014, an associate editor of *IEICE Transactions on Fundamentals of Electronics, Communications and Computer Sciences (IEICE-EA)* in 2015–2018, and an editor of *IEICE-EA* in 2019–2021. He is a member of IEEE and IEICE.



**Ryo Saito** received B.E. and M.E. degrees in Electrical and Computer Engineering from Yokohama National University in 2017 and 2019, respectively. He joined Murata Manufacturing Co., Ltd. and is currently working on research of millimeter wave wireless communications. His research interests include FMCW-MIMO radar and location estimation techniques.



**Daichi Ueki** received B.E. and M.E. degrees in Industrial and Systems Engineering from Keio University in 2011 and 2013, respectively. He joined Murata Manufacturing Co., Ltd. and is currently working on research of millimeter wave wireless communications. His research interests include FMCW-MIMO radar and vital sensing.